Korean Journal of Radiology

KJR

Check for updates

Diffusion-Weighted MRI for the Assessment of Molecular Prognostic Biomarkers in Breast Cancer

Mami Iima[1,2], Masako Kataoka[2], Maya Honda[2,3], Denis Le Bihan[4]

[1]Department of Fundamental Development for Advanced Low Invasive Diagnostic Imaging, Nagoya University Graduate School of Medicine, Nagoya, Japan
[2]Department of Diagnostic Imaging and Nuclear Medicine, Kyoto University Graduate School of Medicine, Kyoto, Japan
[3]Department of Diagnostic Radiology, Kansai Electric Power Hospital, Osaka, Japan
[4]NeuroSpin, Joliot Institute, Department of Fundamental Research, Commissariat à l'Energie Atomique (CEA)-Saclay, Gif-sur-Yvette, France

This study systematically reviewed the role of diffusion-weighted imaging (DWI) in the assessment of molecular prognostic biomarkers in breast cancer, focusing on the correlation of apparent diffusion coefficient (ADC) with hormone receptor status and prognostic biomarkers. Our meta-analysis includes data from 52 studies examining ADC values in relation to estrogen receptor (ER), progesterone receptor (PgR), human epidermal growth factor receptor 2 (HER2), and Ki-67 status. The results indicated significant differences in ADC values among different receptor statuses, with ER-positive, PgR-positive, HER2-negative, and Ki-67-positive tumors having lower ADC values compared to their negative counterparts. This study also highlights the potential of advanced DWI techniques such as intravoxel incoherent motion and non-Gaussian DWI to provide additional insights beyond ADC. Despite these promising findings, the high heterogeneity among the studies underscores the need for standardized DWI protocols to improve their clinical utility in breast cancer management.
Keywords: Breast cancer; Apparent diffusion coefficient; Estrogen receptor; Progesterone receptor; HER-2; Ki-67

INTRODUCTION

Diffusion-weighted imaging (DWI), with more than 35 years of development, provides microstructural and functional information that complements the excellent anatomical details provided by MRI. Although dynamic contrast-enhanced breast MRI can detect malignancies with high sensitivity, its specificity is variable. It also requires the administration of a gadolinium contrast agent, which can cause nephrogenic systemic fibrosis in patients with renal dysfunction, possible tissue deposition with unknown long-term side effects, and contraindications in specific

populations like pregnant women [1].

DWI enables the detection of lesions based on tissue microstructural features revealed by the diffusion of water molecules. The apparent diffusion coefficient (ADC), which eliminates the confounding T1 and T2 effects visible on DW images and provides a quantitative estimation of the water diffusion process in tissues, has been useful for differentiating between benign and malignant breast lesions [2]. Generally, DWI provides outstanding image contrast that reflects the architecture of cancer-specific tissue. Recent advances in MRI gradient hardware have enabled the study of diffusion time-dependent ADCs [3]. Within structured environments, such as cancers, interactions with barriers occur more frequently, thereby reducing the ADC. This makes time-dependent DWI particularly effective for cancer characterization.

Recently, the use of DWI as a complementary and potential alternative imaging technique for evaluating breast lesions has increased. In particular, DWI can provide information in vivo at a microscopic scale, even though DWI data are acquired at the millimeter scale in the form of an ADC that reflects the specific tissue features of cancer

[4,5]. Breast DWI has many advantages that complement conventional breast MRI, thereby improving breast cancer diagnostic accuracy (particularly specificity) and reducing unnecessary biopsy rates in suspected cases of breast cancer.

Many radiologists include ADC in breast MRI diagnostic reports [6], although this parameter has not yet been included in the Breast Imaging Reporting and Data System (BI-RADS). There is a growing interest in making DWI a routine sequence in BI-RADS. However, the use of an ADC with specific cutoff values requires hospitals and institutions to standardize breast DWI or at least meet a minimum level of quality assurance. For these reasons, consensus and recommendations have been published by the International Breast DWI Working Group of the European Society of Breast Imaging [7] and Korean radiologists [8]. Some multicenter studies have revealed that the ADC has the potential to spare patients from unnecessary biopsies for breast cancer diagnosis [9,10], thus reducing patient anxiety and healthcare costs.

As numerous studies have highlighted, ADC is also pivotal in distinguishing hormone receptor statuses and prognostic biomarkers in breast cancer [11], particularly the estrogen receptor (ER), progesterone receptor (PgR), human epidermal growth factor receptor 2 (HER2), and the marker of proliferation Ki-67. In this context, we present a focused and comprehensive summary of evidence regarding the relationship between ADC and the status of crucial ER, PgR, HER-2, and Ki-67 biomarkers in breast cancer. Additionally, we discuss the use of DWI to determine hormone receptor status in breast cancer.

Relationship between ADC and Hormone Receptor Status of Breast Cancer

For a comprehensive, quantitative summary of the relevant data in the literature, we conducted a systematic review and meta-analysis following the guidelines of the Preferred Reporting Items for Systematic Reviews and Meta-Analyses
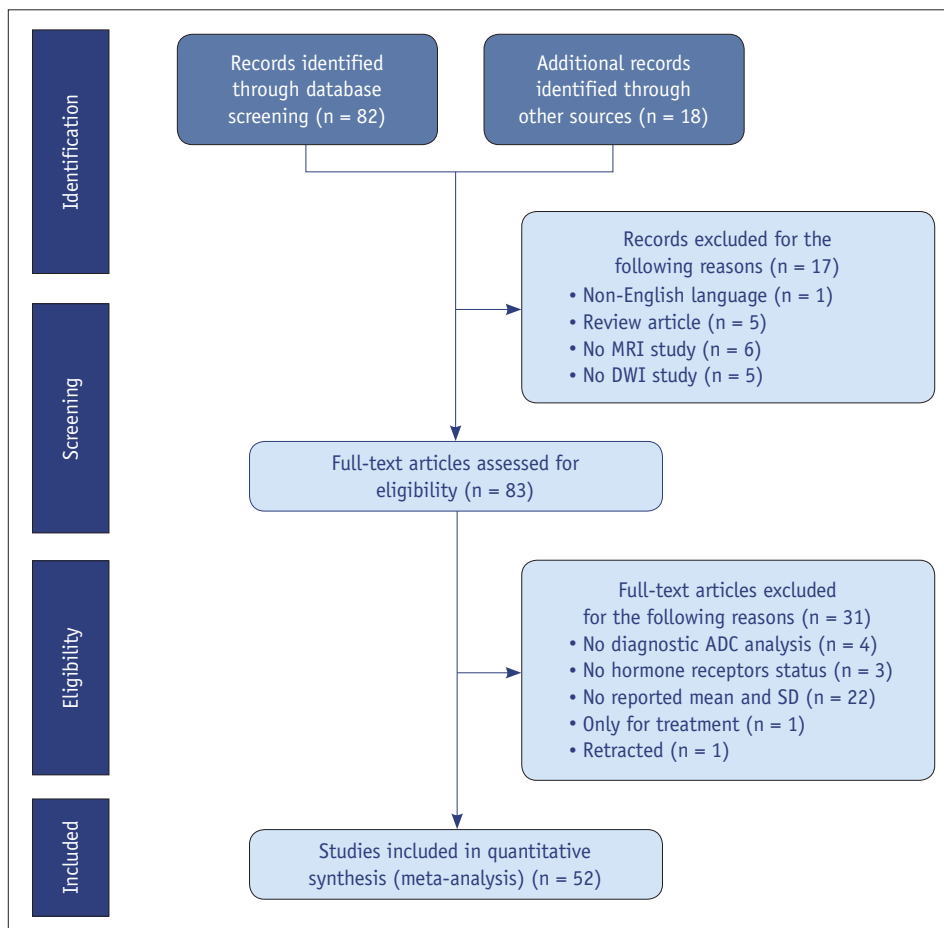

Fig. 1. Flowchart of the screening process for the meta-analysis. MRI = magnetic resonance imaging, DWI = diffusion-weighted imaging, ADC = apparent diffusion coefficient, SD = standard deviation

(PRISMA) statement. The following words were searched using the PubMed, Web of Science, and Google Scholar databases: "breast neoplasm or breast cancer or breast tumor" and "diffusion weighted MRI or diffusion-weighted imaging or diffusion weighted imaging or ADC or apparent diffusion coefficient" and "estrogen receptor or progesterone receptor" or "ER" or "PgR" or "human epidermal growth factor receptor 2" or "HER2 or HER-2." We limited our search to English-language publications and data published between January 2008 and July 2023. The references cited by the relevant articles were manually scanned to search for other pertinent studies.

Two investigators selected eligible studies, and relevant data were independently extracted from the retrieved papers. The results from each study were examined cooperatively and a consensus was reached on all items through discussion and reexamination. All the authors approved the final decision regarding the studies to be admitted. The standardized mean difference in ADC with a 95% confidence interval was used as a summary statistic for ER, PgR, and HER2 categories. A total of 52 articles [3,12-62] were finally reviewed and quantitatively summarized (Fig. 1).

ADCs for Differentiation of ER Status

A forest plot of the mean differences in ADCs between ER-positive and -negative breast cancers from 44 studies [3,13,14,16-22,24,26-38,41-54,56-61] is given in Figure 2A. There was large heterogeneity among the studies ($I^2 = 80\%$), but overall, ER-positive cancers exhibited significantly lower ADCs than ER-negative cancers ($P < 0.01$).

ADCs for Differentiation of PgR Status

A forest plot of the mean difference in ADCs between PgR-positive and -negative breast cancers from 41 studies [3,13,14,16-22,24,26-37,41-43,45-51,53,54,56-61] is provided in Figure 2B. It also showed large heterogeneity across the studies ($I^2 = 80\%$), but overall, PgR-positive cancers had significantly lower ADCs than PgR-negative cancers ($P < 0.01$).

ADCs for Differentiation of HER2 Status

A forest plot of the mean difference in ADCs between HER2-negative and positive cancers from 40 studies [3,15-18,20,21,24-29,31-34,36-38,41-54,56-61] is given in Figure 3A. Again, this showed a large heterogeneity across the studies ($I^2 = 92\%$). Overall, these results showed that HER2-negative cancers had significantly lower ADCs than

HER2-positive cancers ($P < 0.01$).

ADCs for Differentiation of Ki-67 Status

A forest plot of the mean difference in ADCs between Ki-67-positive and -negative cancers from 41 studies [3,12-18,20,21,23,24,26-28,31-40,42,43,45-48,51-55,57,59-62] is given in Figure 3B and shows that Ki-67-positive cancers have significantly lower ADCs than cancers with a negative Ki-67 status ($P < 0.01$), although a large heterogeneity was observed ($I^2 = 94\%$).

Clinical examples of different ER, PgR, HER2, and Ki-67 statuses are shown in Figure 4.

ADCs for Differentiation of Breast Cancer Subtypes

The use of ADCs for the differentiation of breast cancer subtypes has yielded mixed findings, and a meta-analysis has shown that ADC cannot differentiate between breast cancer subtypes [63]. Further investigation is required to verify these results.

ADCs for Cancer Diagnosis, Predicting Treatment Response, and Prognosis

These results show that ER-positivity, PgR-positivity, and HER2-negativity are all related to lower ADC values, although there was a high degree of heterogeneity across the studies. Regarding the relationship between ADC and Ki-67 status, the overall results are consistent with recent clinical and preclinical studies showing that changes in ADC at different diffusion times may provide information on Ki-67 status [3,64] and suggesting that Ki-67 is a useful marker of tissue proliferation at a microscopic scale. In contrast, other studies have reported mixed results regarding the ability of ADCs to differentiate between high and low expression levels of the nuclear protein Ki-67 in breast cancer [2], and a recent multicenter study revealed a relatively low diagnostic performance (AUC: 0.6) of ADCs in such cases [11]. One reason for the variability in these findings might be the differing thresholds for considering Ki-67 as positive in breast cancer, which range from 10% to 50% [11]. Further research is needed to improve the accuracy and reliability of ADC-based differentiation of the Ki-67 status. In addition, although our meta-analysis elucidated the correlations between ADC values and the status of hormone receptors, including ER, PgR, HER2, and Ki-67 in breast cancer, the precise effect size of these correlations remains to be definitively established, warranting further research for more conclusive insights. Corrections based on the lesion
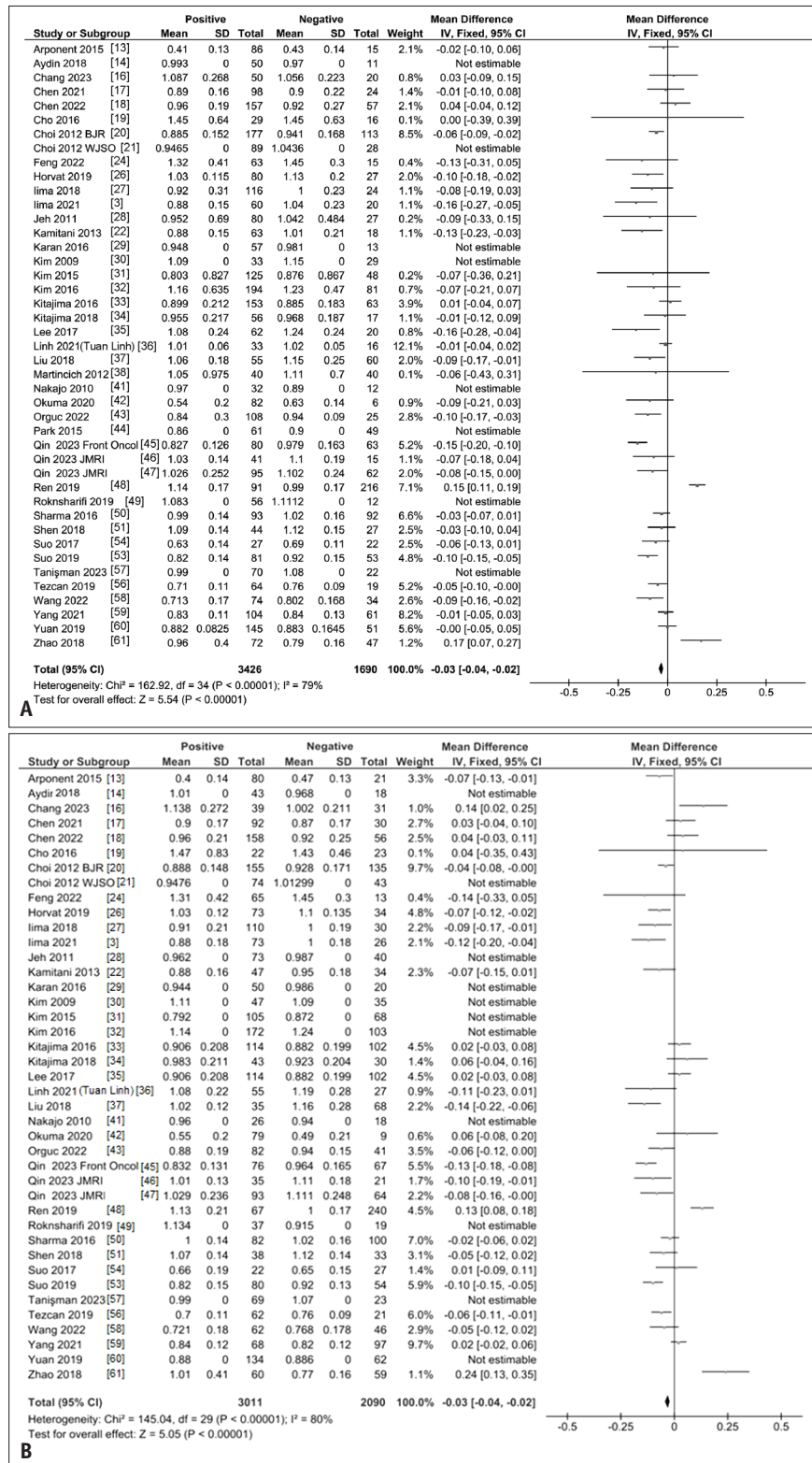
A

Study or Subgroup	Positive Mean	SD	Total	Negative Mean	SD	Total	Weight	Mean Difference IV, Fixed, 95% CI
Arponent 2015 [13]	0.41	0.13	86	0.43	0.14	15	2.1%	-0.02 [-0.10, 0.06]
Aydin 2018 [14]	0.993	0	50	0.97	0	11		Not estimable
Chang 2023 [16]	1.087	0.268	50	1.056	0.223	20	0.8%	0.03 [-0.09, 0.15]
Chen 2021 [17]	0.89	0.16	98	0.9	0.22	24	1.4%	-0.01 [-0.10, 0.08]
Chen 2022 [18]	0.96	0.19	157	0.92	0.27	57	2.1%	0.04 [-0.04, 0.12]
Cho 2016 [19]	1.45	0.64	29	1.45	0.63	16	0.1%	0.00 [-0.39, 0.39]
Choi 2012 BJR [20]	0.885	0.152	177	0.941	0.168	113	8.5%	-0.06 [-0.09, -0.02]
Choi 2012 WJSO [21]	0.9465	0	89	1.0436	0	28		Not estimable
Feng 2022 [24]	1.32	0.41	63	1.45	0.3	15	0.4%	-0.13 [-0.31, 0.05]
Horvat 2019 [26]	1.03	0.115	80	1.13	0.2	27	2.0%	-0.10 [-0.18, -0.02]
Iima 2018 [27]	0.92	0.31	116	1	0.23	24	1.1%	-0.08 [-0.19, 0.03]
Iima 2021 [3]	0.88	0.15	60	1.04	0.23	20	1.1%	-0.16 [-0.27, -0.05]
Jeh 2011 [28]	0.952	0.69	80	1.042	0.484	27	0.2%	-0.09 [-0.33, 0.15]
Kamitani 2013 [22]	0.88	0.15	63	1.01	0.21	18	1.1%	-0.13 [-0.23, -0.03]
Karan 2016 [29]	0.948	0	57	0.981	0	13		Not estimable
Kim 2009 [30]	1.09	0	33	1.15	0	29		Not estimable
Kim 2015 [31]	0.803	0.827	125	0.876	0.867	48	0.2%	-0.07 [-0.36, 0.21]
Kim 2016 [32]	1.16	0.635	194	1.23	0.47	81	0.7%	-0.07 [-0.21, 0.07]
Kitajima 2016 [33]	0.899	0.212	153	0.885	0.183	63	3.9%	0.01 [-0.04, 0.07]
Kitajima 2018 [34]	0.955	0.217	56	0.968	0.187	17	1.1%	-0.01 [-0.12, 0.09]
Lee 2017 [35]	1.08	0.24	62	1.24	0.24	20	0.8%	-0.16 [-0.28, -0.04]
Linh 2021(Tuan Linh) [36]	1.01	0.06	33	1.02	0.05	16	12.1%	-0.01 [-0.04, 0.02]
Liu 2018 [37]	1.06	0.18	55	1.15	0.25	60	2.0%	-0.09 [-0.17, -0.01]
Martincich 2012 [38]	1.05	0.975	40	1.11	0.7	40	0.1%	-0.06 [-0.43, 0.31]
Nakajo 2010 [41]	0.97	0	32	0.89	0	12		Not estimable
Okuma 2020 [42]	0.54	0.2	82	0.63	0.14	6	0.9%	-0.09 [-0.21, 0.03]
Orguc 2022 [43]	0.84	0.3	108	0.94	0.09	25	2.8%	-0.10 [-0.17, -0.03]
Park 2015 [44]	0.86	0	61	0.9	0	49		Not estimable
Qin 2023 Front Oncol [45]	0.827	0.126	80	0.979	0.163	63	5.2%	-0.15 [-0.20, -0.10]
Qin 2023 JMRI [46]	1.03	0.14	41	1.1	0.19	15	1.1%	-0.07 [-0.18, 0.04]
Qin 2023 JMRI [47]	1.026	0.252	95	1.102	0.24	62	2.0%	-0.08 [-0.15, 0.00]
Ren 2019 [48]	1.14	0.17	91	0.99	0.17	216	7.1%	0.15 [0.11, 0.19]
Roknsharifi 2019 [49]	1.083	0	56	1.1112	0	12		Not estimable
Sharma 2016 [50]	0.99	0.14	93	1.02	0.16	92	6.6%	-0.03 [-0.07, 0.01]
Shen 2018 [51]	1.09	0.14	44	1.12	0.15	27	2.5%	-0.03 [-0.10, 0.04]
Suo 2017 [54]	0.63	0.14	27	0.69	0.11	22	2.5%	-0.06 [-0.13, 0.01]
Suo 2019 [53]	0.82	0.14	81	0.92	0.15	53	4.8%	-0.10 [-0.15, -0.05]
Tanişman 2023 [57]	0.99	0	70	1.08	0	22		Not estimable
Tezcan 2019 [56]	0.71	0.11	64	0.76	0.09	19	5.2%	-0.05 [-0.10, -0.00]
Wang 2022 [58]	0.713	0.17	74	0.802	0.168	34	2.6%	-0.09 [-0.16, -0.02]
Yang 2021 [59]	0.83	0.11	104	0.84	0.13	61	8.2%	-0.01 [-0.05, 0.03]
Yuan 2019 [60]	0.882	0.0825	145	0.883	0.1645	51	5.6%	-0.00 [-0.05, 0.05]
Zhao 2018 [61]	0.96	0.4	72	0.79	0.16	47	1.2%	0.17 [0.07, 0.27]
Total (95% CI)			**3426**			**1690**	**100.0%**	**-0.03 [-0.04, -0.02]**

Heterogeneity: Chi² = 162.92, df = 34 (P < 0.00001); I² = 79%
Test for overall effect: Z = 5.54 (P < 0.00001)

B

Study or Subgroup	Positive Mean	SD	Total	Negative Mean	SD	Total	Weight	Mean Difference IV, Fixed, 95% CI
Arponent 2015 [13]	0.4	0.14	80	0.47	0.13	21	3.3%	-0.07 [-0.13, -0.01]
Aydin 2018 [14]	1.01	0	43	0.968	0	18		Not estimable
Chang 2023 [16]	1.138	0.272	39	1.002	0.211	31	1.0%	0.14 [0.02, 0.25]
Chen 2021 [17]	0.9	0.17	92	0.87	0.17	30	2.7%	0.03 [-0.04, 0.10]
Chen 2022 [18]	0.96	0.21	158	0.92	0.25	56	2.5%	0.04 [-0.03, 0.11]
Cho 2016 [19]	1.47	0.83	22	1.43	0.46	23	0.1%	0.04 [-0.35, 0.43]
Choi 2012 BJR [20]	0.888	0.148	155	0.928	0.171	135	9.7%	-0.04 [-0.08, -0.00]
Choi 2012 WJSO [21]	0.9476	0	74	1.01299	0	43		Not estimable
Feng 2022 [24]	1.31	0.42	65	1.45	0.3	13	0.4%	-0.14 [-0.33, 0.05]
Horvat 2019 [26]	1.03	0.12	73	1.1	0.135	34	4.8%	-0.07 [-0.12, -0.02]
Iima 2018 [27]	0.91	0.21	110	1	0.19	30	2.2%	-0.09 [-0.17, -0.01]
Iima 2021 [3]	0.88	0.18	73	1	0.18	26	2.1%	-0.12 [-0.20, -0.04]
Jeh 2011 [28]	0.962	0	73	0.987	0	40		Not estimable
Kamitani 2013 [22]	0.88	0.16	47	0.95	0.18	34	2.3%	-0.07 [-0.15, 0.01]
Karan 2016 [29]	0.944	0	50	0.986	0	20		Not estimable
Kim 2009 [30]	1.11	0	47	1.09	0	35		Not estimable
Kim 2015 [31]	0.792	0	105	0.872	0	68		Not estimable
Kim 2016 [32]	1.14	0	172	1.24	0	103		Not estimable
Kitajima 2016 [33]	0.906	0.208	114	0.882	0.199	102	4.5%	0.02 [-0.03, 0.08]
Kitajima 2018 [34]	0.983	0.211	43	0.923	0.204	30	1.4%	0.06 [-0.04, 0.16]
Lee 2017 [35]	0.906	0.208	114	0.882	0.199	102	4.5%	0.02 [-0.03, 0.08]
Linh 2021 (Tuan Linh) [36]	1.08	0.22	55	1.19	0.28	27	0.9%	-0.11 [-0.23, 0.01]
Liu 2018 [37]	1.02	0.12	35	1.16	0.28	68	2.2%	-0.14 [-0.22, -0.06]
Nakajo 2010 [41]	0.96	0	26	0.94	0	18		Not estimable
Okuma 2020 [42]	0.55	0.2	79	0.49	0.21	9	0.6%	0.06 [-0.08, 0.20]
Orguc 2022 [43]	0.88	0.19	82	0.94	0.15	41	3.5%	-0.06 [-0.12, 0.00]
Qin 2023 Front Oncol [45]	0.832	0.131	76	0.964	0.165	67	5.5%	-0.13 [-0.18, -0.08]
Qin 2023 JMRI [46]	1.01	0.13	35	1.11	0.18	21	1.7%	-0.10 [-0.19, -0.01]
Qin 2023 JMRI [47]	1.029	0.236	93	1.111	0.248	64	2.2%	-0.08 [-0.16, -0.00]
Ren 2019 [48]	1.13	0.21	67	1	0.17	240	4.5%	0.13 [0.08, 0.18]
Roknsharifi 2019 [49]	1.134	0	37	0.915	0	19		Not estimable
Sharma 2016 [50]	1	0.14	82	1.02	0.16	100	7.0%	-0.02 [-0.06, 0.02]
Shen 2018 [51]	1.07	0.14	38	1.12	0.14	33	3.1%	-0.05 [-0.12, 0.02]
Suo 2017 [54]	0.66	0.19	22	0.65	0.15	27	1.4%	0.01 [-0.09, 0.11]
Suo 2019 [53]	0.82	0.14	80	0.92	0.13	54	5.9%	-0.10 [-0.15, -0.05]
Tanişman 2023 [57]	0.99	0	69	1.07	0	23		Not estimable
Tezcan 2019 [56]	0.7	0.11	62	0.76	0.09	21	6.0%	-0.06 [-0.11, -0.01]
Wang 2022 [58]	0.721	0.18	62	0.768	0.178	46	2.9%	-0.05 [-0.12, 0.02]
Yang 2021 [59]	0.84	0.12	68	0.82	0.12	97	9.7%	0.02 [-0.02, 0.06]
Yuan 2019 [60]	0.88	0	134	0.886	0	62		Not estimable
Zhao 2018 [61]	1.01	0.41	60	0.77	0.16	59	1.1%	0.24 [0.13, 0.35]
Total (95% CI)			**3011**			**2090**	**100.0%**	**-0.03 [-0.04, -0.02]**

Heterogeneity: Chi² = 145.04, df = 29 (P < 0.00001); I² = 80%
Test for overall effect: Z = 5.05 (P < 0.00001)

Fig. 2. ADC differences in breast tumors by hormone receptor status. **A:** A forest plot of mean ADC (10^{-3} mm²/s) difference reported for ER-positive and ER-negative breast tumors. Tumors with positive ER status have significantly lower ADCs compared with receptor-negative tumors. **B:** Forest plot of mean ADC (10^{-3} mm²/s) difference reported for PgR-positive and PgR-negative breast tumors. Tumors with positive PgR status exhibit significantly lower ADCs compared with PgR-negative tumors. ADC = apparent diffusion coefficient, ER = estrogen receptor, PgR = progesterone receptor, SD = standard deviation, IV = weighted mean difference, CI = confidence interval, Chi² = chi-squared test statistic, df = degrees of freedom, I² = heterogeneity statistic, Z = Z-test statistic
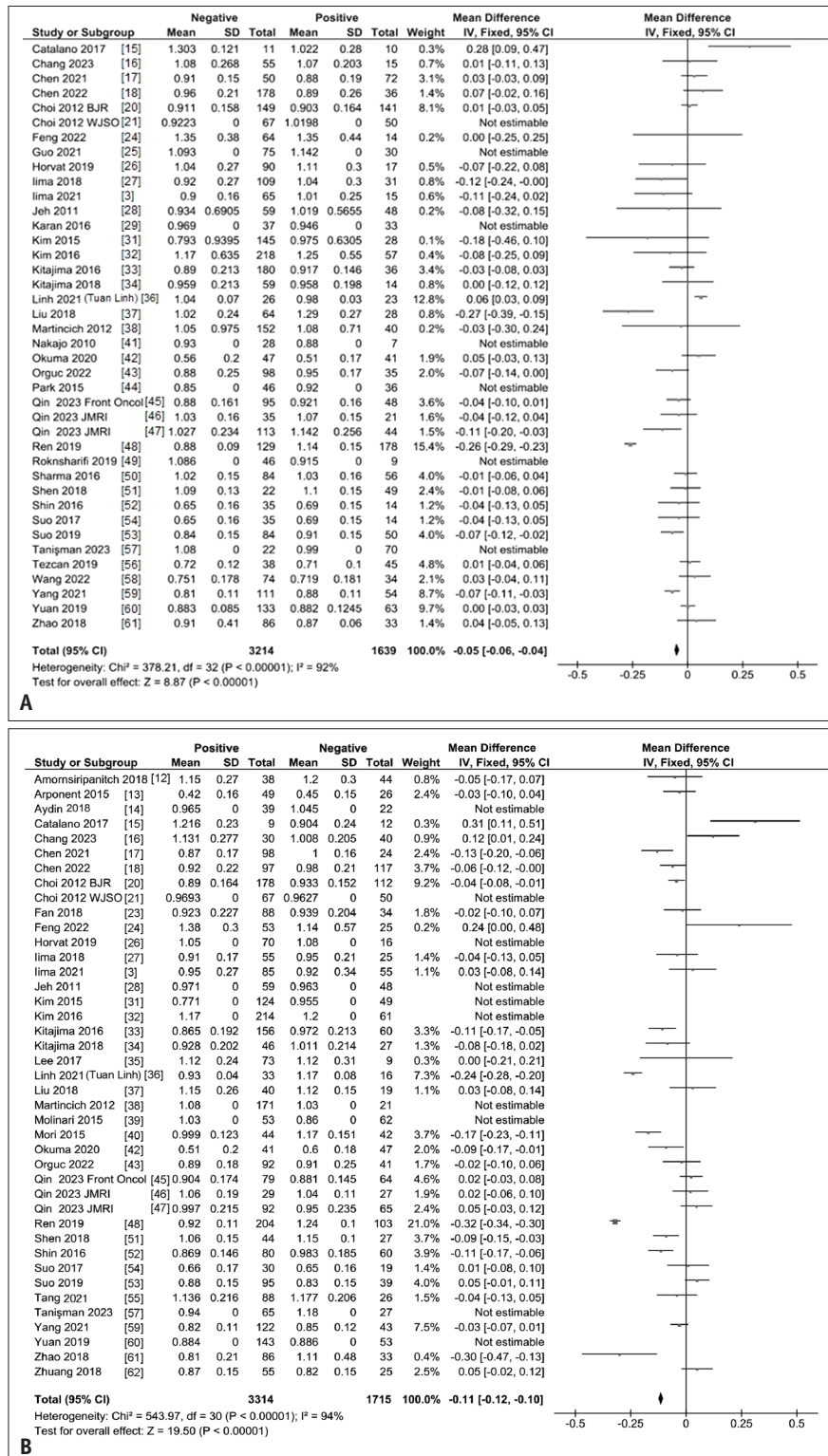
A

Study or Subgroup	Negative Mean	SD	Total	Positive Mean	SD	Total	Weight	Mean Difference IV, Fixed, 95% CI
Catalano 2017 [15]	1.303	0.121	11	1.022	0.28	10	0.3%	0.28 [0.09, 0.47]
Chang 2023 [16]	1.08	0.268	55	1.07	0.203	15	0.7%	0.01 [-0.11, 0.13]
Chen 2021 [17]	0.91	0.15	50	0.88	0.19	72	3.1%	0.03 [-0.03, 0.09]
Chen 2022 [18]	0.96	0.21	178	0.89	0.26	36	1.4%	0.07 [-0.02, 0.16]
Choi 2012 BJR [20]	0.911	0.158	149	0.903	0.164	141	8.1%	0.01 [-0.03, 0.05]
Choi 2012 WJSO [21]	0.9223	0	67	1.0198	0	50		Not estimable
Feng 2022 [24]	1.35	0.38	64	1.35	0.44	14	0.2%	0.00 [-0.25, 0.25]
Guo 2021 [25]	1.093	0	75	1.142	0	30		Not estimable
Horvat 2019 [26]	1.04	0.27	90	1.11	0.3	17	0.5%	-0.07 [-0.22, 0.08]
Iima 2018 [27]	0.92	0.27	109	1.04	0.3	31	0.8%	-0.12 [-0.24, -0.00]
Iima 2021 [3]	0.9	0.16	65	1.01	0.25	15	0.6%	-0.11 [-0.24, 0.02]
Jeh 2011 [28]	0.934	0.6905	59	1.019	0.5655	48	0.2%	-0.08 [-0.32, 0.15]
Karan 2016 [29]	0.969	0	37	0.946	0	33		Not estimable
Kim 2015 [31]	0.793	0.9395	145	0.975	0.6305	28	0.1%	-0.18 [-0.46, 0.10]
Kim 2016 [32]	1.17	0.635	218	1.25	0.55	57	0.4%	-0.08 [-0.25, 0.09]
Kitajima 2016 [33]	0.89	0.213	180	0.917	0.146	36	3.4%	-0.03 [-0.08, 0.03]
Kitajima 2018 [34]	0.959	0.213	59	0.958	0.198	14	0.8%	0.00 [-0.12, 0.12]
Linh 2021 (Tuan Linh) [36]	1.04	0.07	26	0.98	0.03	23	12.8%	0.06 [0.03, 0.09]
Liu 2018 [37]	1.02	0.24	64	1.29	0.27	28	0.8%	-0.27 [-0.39, -0.15]
Martincich 2012 [38]	1.05	0.975	152	1.08	0.71	40	0.2%	-0.03 [-0.30, 0.24]
Nakajo 2010 [41]	0.93	0	28	0.88	0	7		Not estimable
Okuma 2020 [42]	0.56	0.2	47	0.51	0.17	41	1.9%	0.05 [-0.03, 0.13]
Orguc 2022 [43]	0.88	0.25	98	0.95	0.17	35	2.0%	-0.07 [-0.14, 0.00]
Park 2015 [44]	0.85	0	46	0.92	0	36		Not estimable
Qin 2023 Front Oncol [45]	0.88	0.161	95	0.921	0.16	48	3.6%	-0.04 [-0.10, 0.01]
Qin 2023 JMRI [46]	1.03	0.16	35	1.07	0.15	21	1.6%	-0.04 [-0.12, 0.04]
Qin 2023 JMRI [47]	1.027	0.234	113	1.142	0.256	44	1.5%	-0.11 [-0.20, -0.03]
Ren 2019 [48]	0.88	0.09	129	1.14	0.15	178	15.4%	-0.26 [-0.29, -0.23]
Roknsharifi 2019 [49]	1.086	0	46	0.915	0	9		Not estimable
Sharma 2016 [50]	1.02	0.15	84	1.03	0.16	56	4.0%	-0.01 [-0.06, 0.04]
Shen 2018 [51]	1.09	0.13	22	1.1	0.15	49	2.4%	-0.01 [-0.08, 0.06]
Shin 2016 [52]	0.65	0.16	35	0.69	0.15	14	1.2%	-0.04 [-0.13, 0.05]
Suo 2017 [54]	0.65	0.16	35	0.69	0.15	14	1.2%	-0.04 [-0.13, 0.05]
Suo 2019 [53]	0.84	0.15	84	0.91	0.15	50	4.0%	-0.07 [-0.12, -0.02]
Tanışman 2023 [57]	1.08	0	22	0.99	0	70		Not estimable
Tezcan 2019 [56]	0.72	0.12	38	0.71	0.1	45	4.8%	0.01 [-0.04, 0.06]
Wang 2022 [58]	0.751	0.178	74	0.719	0.181	34	2.1%	0.03 [-0.04, 0.11]
Yang 2021 [59]	0.81	0.11	111	0.88	0.11	54	8.7%	-0.07 [-0.11, -0.03]
Yuan 2019 [60]	0.883	0.085	133	0.882	0.1245	63	9.7%	0.00 [-0.03, 0.03]
Zhao 2018 [61]	0.91	0.41	86	0.87	0.06	33	1.4%	0.04 [-0.05, 0.13]
Total (95% CI)			**3214**			**1639**	**100.0%**	**-0.05 [-0.06, -0.04]**

Heterogeneity: Chi² = 378.21, df = 32 (P < 0.00001); I² = 92%
Test for overall effect: Z = 8.87 (P < 0.00001)

B

Study or Subgroup	Positive Mean	SD	Total	Negative Mean	SD	Total	Weight	Mean Difference IV, Fixed, 95% CI
Amornsiripanitch 2018 [12]	1.15	0.27	38	1.2	0.3	44	0.8%	-0.05 [-0.17, 0.07]
Arponent 2015 [13]	0.42	0.16	49	0.45	0.15	26	2.4%	-0.03 [-0.10, 0.04]
Aydin 2018 [14]	0.965	0	39	1.045	0	22		Not estimable
Catalano 2017 [15]	1.216	0.23	9	0.904	0.24	12	0.3%	0.31 [0.11, 0.51]
Chang 2023 [16]	1.131	0.277	30	1.008	0.205	40	0.9%	0.12 [0.01, 0.24]
Chen 2021 [17]	0.87	0.17	98	1	0.16	24	2.4%	-0.13 [-0.20, -0.06]
Chen 2022 [18]	0.92	0.22	97	0.98	0.21	117	3.7%	-0.06 [-0.12, -0.00]
Choi 2012 BJR [20]	0.89	0.164	178	0.933	0.152	112	9.2%	-0.04 [-0.08, -0.01]
Choi 2012 WJSO [21]	0.9693	0	67	0.9627	0	50		Not estimable
Fan 2018 [23]	0.923	0.227	88	0.939	0.204	34	1.8%	-0.02 [-0.10, 0.07]
Feng 2022 [24]	1.38	0.3	53	1.14	0.57	25	0.2%	0.24 [0.00, 0.48]
Horvat 2019 [26]	1.05	0	70	1.08	0	16		Not estimable
Iima 2018 [27]	0.91	0.17	55	0.95	0.21	25	1.4%	-0.04 [-0.13, 0.05]
Iima 2021 [3]	0.95	0.27	85	0.92	0.34	55	1.1%	0.03 [-0.08, 0.14]
Jeh 2011 [28]	0.971	0	59	0.963	0	48		Not estimable
Kim 2015 [31]	0.771	0	124	0.955	0	49		Not estimable
Kim 2016 [32]	1.17	0	214	1.2	0	61		Not estimable
Kitajima 2016 [33]	0.865	0.192	156	0.972	0.213	60	3.3%	-0.11 [-0.17, -0.05]
Kitajima 2018 [34]	0.928	0.202	46	1.011	0.214	27	1.3%	-0.08 [-0.18, 0.02]
Lee 2017 [35]	1.12	0.24	73	1.12	0.31	9	0.3%	0.00 [-0.21, 0.21]
Linh 2021 (Tuan Linh) [36]	0.93	0.04	33	1.17	0.08	16	7.3%	-0.24 [-0.28, -0.20]
Liu 2018 [37]	1.15	0.26	40	1.12	0.15	19	1.1%	0.03 [-0.08, 0.14]
Martincich 2012 [38]	1.08	0	171	1.03	0	21		Not estimable
Molinari 2015 [39]	1.03	0	53	0.86	0	62		Not estimable
Mori 2015 [40]	0.999	0.123	44	1.17	0.151	42	3.7%	-0.17 [-0.23, -0.11]
Okuma 2020 [42]	0.51	0.2	41	0.6	0.18	47	2.0%	-0.09 [-0.17, -0.01]
Orguc 2022 [43]	0.89	0.18	92	0.91	0.25	41	1.7%	-0.02 [-0.10, 0.06]
Qin 2023 Front Oncol [45]	0.904	0.174	79	0.881	0.145	64	4.6%	0.02 [-0.03, 0.08]
Qin 2023 JMRI [46]	1.06	0.19	29	1.04	0.11	27	1.9%	0.02 [-0.06, 0.10]
Qin 2023 JMRI [47]	0.997	0.215	92	0.95	0.235	65	2.4%	0.05 [-0.03, 0.12]
Ren 2019 [48]	0.92	0.11	204	1.24	0.1	103	21.0%	-0.32 [-0.34, -0.30]
Shen 2018 [51]	1.06	0.15	44	1.15	0.1	27	3.7%	-0.09 [-0.15, -0.03]
Shin 2016 [52]	0.869	0.146	80	0.983	0.185	60	3.9%	-0.11 [-0.17, -0.06]
Suo 2017 [54]	0.66	0.17	30	0.65	0.16	19	1.4%	0.01 [-0.08, 0.10]
Suo 2019 [53]	0.88	0.15	95	0.83	0.15	39	4.0%	0.05 [-0.01, 0.11]
Tang 2021 [55]	1.136	0.216	88	1.177	0.206	26	1.5%	-0.04 [-0.13, 0.05]
Tanışman 2023 [57]	0.94	0	65	1.18	0	27		Not estimable
Yang 2021 [59]	0.82	0.11	122	0.85	0.12	43	7.5%	-0.03 [-0.07, 0.01]
Yuan 2019 [60]	0.884	0	143	0.886	0	53		Not estimable
Zhao 2018 [61]	0.81	0.21	86	1.11	0.48	33	0.4%	-0.30 [-0.47, -0.13]
Zhuang 2018 [62]	0.87	0.15	55	0.82	0.15	25	2.5%	0.05 [-0.02, 0.12]
Total (95% CI)			**3314**			**1715**	**100.0%**	**-0.11 [-0.12, -0.10]**

Heterogeneity: Chi² = 543.97, df = 30 (P < 0.00001); I² = 94%
Test for overall effect: Z = 19.50 (P < 0.00001)

Fig. 3. ADC differences in breast tumors by HER2 status and Ki-67 status. **A:** Forest plot of mean ADC (10^{-3} mm²/s) difference reported for breast tumors with negative and positive HER2 status. Tumors exhibiting negative HER2 status show significantly lower ADCs than those with positive HER2 status. **B:** Forest plot of mean ADC (10^{-3} mm²/s) difference reported for markers of proliferation Ki-67-positive and Ki-67-negative breast tumors. Tumors positive for Ki-67 show significantly lower ADCs compared to those with negative Ki-67 status. ADC = apparent diffusion coefficient, HER2 = human epidermal growth factor 2 receptor, SD = standard deviation, IV = weighted mean difference, CI = confidence interval, Chi² = chi-squared test statistic, df = degrees of freedom, I² = heterogeneity statistic, Z = Z-test statistic

			ADC (x 10^{-3}/mm²/s)	ER	PgR	HER2	Ki-67
			0.80	-	-	-	+
			0.72	+	+	-	+
			1.16	+	-	-	-
			0.75	-	-	+	+
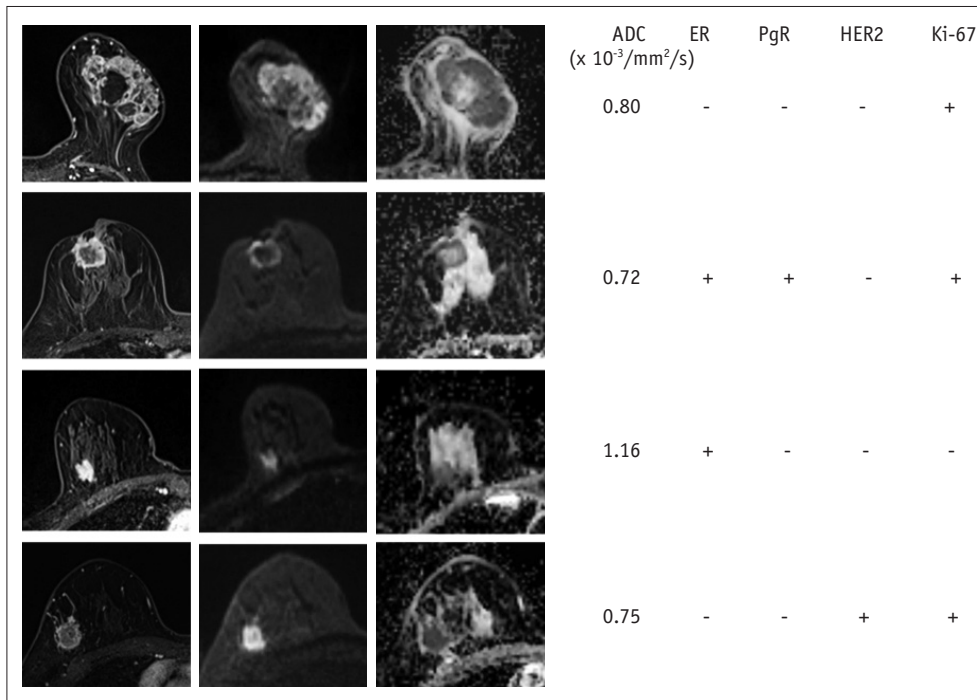
Fig. 4. Clinical examples of breast cancers (invasive ductal carcinomas). Contrast-enhanced images, diffusion-weighted images at a b value of 1000 sec/mm², and ADC maps are shown. The ADC values and each ER, PgR, HER2, and Ki-67 status of breast cancers are also demonstrated. ADC = apparent diffusion coefficient, ER = estrogen receptor, PgR = progesterone receptor, HER-2 = human epidermal growth factor receptor 2

size may be necessary to understand these relationships more accurately.

Specific ADC thresholds could help identify patients at higher risk, leading to a more personalized treatment for breast cancer. These findings pave the way for future studies to better use ADCs to determine the hormone receptor status. However, the interpretation of these results may have been influenced by the chosen diffusion time, histological threshold, and inconsistent acquisition parameters. The high inconsistency among studies, possibly exacerbated by small sample sizes, highlights the critical need for standardization in research methodologies. In addition, small mean differences in ADC values associated with hormone receptor status were observed in this study, which might have been influenced by the heterogeneity of the acquisition protocol. The standardization of ADC values, including reproducibility, is critical for verifying these changes.

Some multicenter studies have revealed that the ADC has the potential to spare patients from unnecessary biopsies for breast cancer diagnosis [9,10], thus reducing patient anxiety and healthcare costs. In addition to diagnosis, the ADC has been investigated as a potential predictor of treatment response in patients with breast cancer. The American College of Radiology Imaging Network conducted a multicenter study to assess the usefulness of ADCs in predicting the response to neoadjuvant chemotherapy in patients with breast cancer [65]. This study revealed that changes in ADCs during treatment could predict a pathological response to neoadjuvant chemotherapy and that mid-treatment changes in ADCs were predictive of hormone receptor-positive/HER2-negative cancers. Predicting treatment responses using the ADC may help guide treatment decisions and avoid ineffective therapies.

Beyond ADC: IVIM and Non-Gaussian DWI

Intravoxel incoherent motion (IVIM) and non-Gaussian DWI can provide additional information on tissue microstructure and microvasculature compared with standard ADC measurements. IVIM can be used to evaluate perfusion in capillaries, primarily at low b values (< 200 s/mm²). Large b values (> 1000 s/mm²) predominantly indicated hindered or restricted diffusion, and the non-normality of DWI could be quantified using the kurtosis model (Fig. 5). The ability to accurately characterize tissue microstructure and microvasculature can enhance the diagnostic accuracy of breast MRI, and IVIM has shown promise in differentiating between malignant and benign breast lesions [66,67].
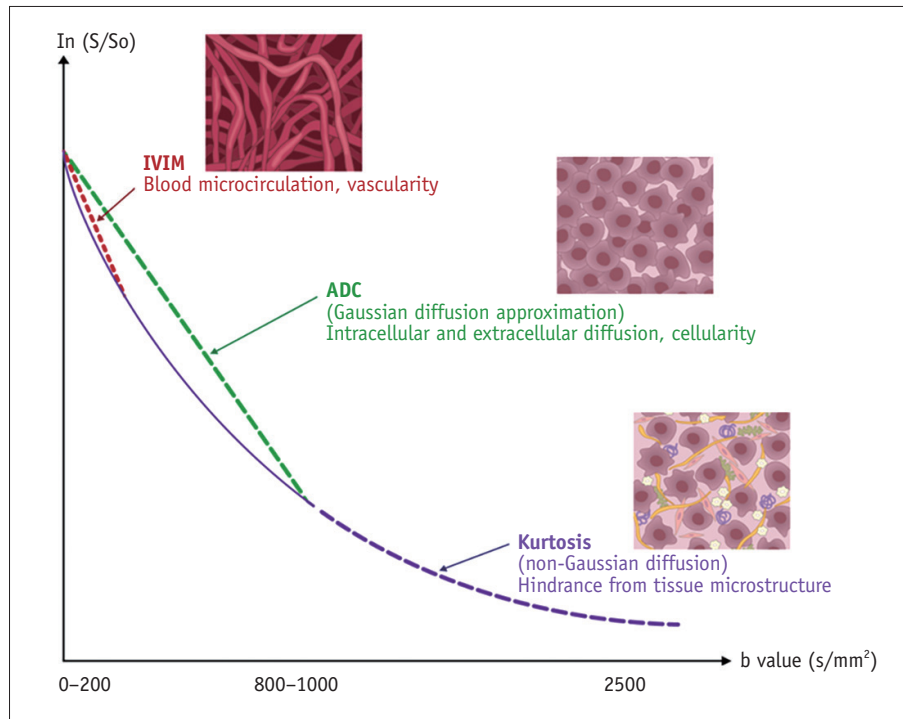
Fig. 5. Example of a diffusion signal decay in typical breast lesions. IVIM offers insights into blood microcirculation and tissue vascularity, whereas the ADC reflects both intracellular and extracellular water diffusion, providing information about tissue cellularity. Kurtosis imaging measures the deviation from Gaussian water diffusion, offering information about hindrances caused by the tissue microstructure. IVIM = intravoxel incoherent motion, ADC = apparent diffusion coefficient

Mean kurtosis values have also been found to be useful for differentiating invasive ductal carcinoma from ductal carcinoma in situ [66]. The difference between the maximum and minimum ADCs, together with the kurtosis value calculated from a non-Gaussian diffusion model, may also help predict metastatic breast cancer [68,69]. While IVIM and non-Gaussian DWI often require the acquisition of large sets of diffusion-weighted images and dedicated data processing, recent approaches have shown that IVIM and non-Gaussian diffusion information can be collected using ad hoc parameters, such as the shifted ADC [4] and signature index [4,70]. The latter, in particular, has been shown to provide information on cancer subtypes and hormone status [71]. However, it is clear that these advanced DWI techniques require standardization in terms of both acquisition and analysis.

CONCLUSION

Breast DWI is a rapidly growing and valuable methodology for detecting and characterizing breast cancer and predicting treatment responses. It is also safe for most women. Although ADCs have been reported to significantly correlate with some molecular prognostic biomarkers and some trends might be evident, as demonstrated in the meta-analysis, there remains a lack of consensus among studies. Additionally, the accuracy of breast cancer diagnosis using DWI may be influenced by the selected diffusion times and histological thresholds, underscoring the need for standardized DWI protocols for breast cancer diagnosis. Accumulating evidence suggests that several alternative measures, including IVIM and non-Gaussian DWI, can serve as useful imaging biomarkers in clinical settings.

Conflicts of Interest
The authors have no potential conflicts of interest to disclose.

Author Contributions
Conceptualization: Mami Iima. Data curation: Mami Iima, Masako Kataoka, Maya Honda. Formal analysis: Mami Iima, Masako Kataoka. Funding acquisition: Mami Iima. Investigation: all authors. Methodology: Mami Iima, Masako Kataoka, Maya Honda. Project administration: Mami Iima, Masako Kataoka. Resources: all authors. Software: Mami Iima, Masako Kataoka, Maya Honda. Supervision: Mami

https://doi.org/10.3348/kjr.2023.1188

Iima, Denis Le Bihan. Validation: all authors. Visualization: all authors. Writing—original draft: Mami Iima, Masako Kataoka, Maya Honda. Writing—review & editing: all authors.

ORCID IDs
Mami Iima
   https://orcid.org/0000-0002-1991-2494
Masako Kataoka
   https://orcid.org/0000-0002-6212-3351
Maya Honda
   https://orcid.org/0000-0002-5337-3455
Denis Le Bihan
   https://orcid.org/0000-0002-4454-729X

REFERENCES

1. Amornsiripanitch N, Bickelhaupt S, Shin HJ, Dang M, Rahbar H, Pinker K, et al. Diffusion-weighted MRI for unenhanced breast cancer screening. *Radiology* 2019;293:504-520

2. Iima M, Honda M, Sigmund EE, Ohno Kishimoto A, Kataoka M, Togashi K. Diffusion MRI of the breast: current status and future directions. *J Magn Reson Imaging* 2020;52:70-90

3. Iima M, Kataoka M, Honda M, Ohashi A, Ohno Kishimoto A, Ota R, et al. The rate of apparent diffusion coefficient change with diffusion time on breast diffusion-weighted imaging depends on breast tumor types and molecular prognostic biomarker expression. *Invest Radiol* 2021;56:501-508

4. Iima M, Le Bihan D. Clinical intravoxel incoherent motion and diffusion MR imaging: past, present, and future. *Radiology* 2016;278:13-32

5. Le Bihan D. Looking into the functional architecture of the brain with diffusion MRI. *Nat Rev Neurosci* 2003;4:469-480

6. Lo Gullo R, Sevilimedu V, Baltzer P, Le Bihan D, Camps-Herrero J, Clauser P, et al. A survey by the European Society of Breast Imaging on the implementation of breast diffusion-weighted imaging in clinical practice. *Eur Radiol* 2022;32:6588-6597

7. Baltzer P, Mann RM, Iima M, Sigmund EE, Clauser P, Gilbert FJ, et al. Diffusion-weighted imaging of the breast-a consensus and mission statement from the EUSOBI international breast diffusion-weighted imaging working group. *Eur Radiol*

2020;30:1436-1450

8. Lee SH, Shin HJ, Moon WK. Diffusion-weighted magnetic resonance imaging of the breast: standardization of image acquisition and interpretation. *Korean J Radiol* 2021;22:9-22

9. Rahbar H, Zhang Z, Chenevert TL, Romanoff J, Kitsch AE, Hanna LG, et al. Utility of diffusion-weighted imaging to decrease unnecessary biopsies prompted by breast MRI: a trial of the ECOG-ACRIN cancer research group (A6702). *Clin Cancer Res* 2019;25:1756-1765

10. Clauser P, Krug B, Bickel H, Dietzel M, Pinker K, Neuhaus VF, et al. Diffusion-weighted imaging allows for downgrading MR BI-RADS 4 lesions in contrast-enhanced MRI of the breast to avoid unnecessary biopsy. *Clin Cancer Res* 2021;27:1941-1948

11. Surov A, Clauser P, Chang YW, Li L, Martincich L, Partridge SC, et al. Can diffusion-weighted imaging predict tumor grade and expression of Ki-67 in breast cancer? A multicenter analysis. *Breast Cancer Res* 2018;20:58

12. Amornsiripanitch N, Nguyen VT, Rahbar H, Hippe DS, Gadi VK, Rendi MH, et al. Diffusion-weighted MRI characteristics associated with prognostic pathological factors and recurrence risk in invasive ER+/HER2- breast cancers. *J Magn Reson Imaging* 2018;48:226-236

13. Arponent O, Sudah M, Masarwah A, Taina M, Rautiainen S, Könönen M, et al. Diffusion-weighted imaging in 3.0 tesla breast MRI: diagnostic performance and tumor characterization using small subregions vs. whole tumor regions of interest. *PLoS One* 2015;10:e0138702

14. Aydin H, Guner B, Esen Bostanci I, Bulut ZM, Aribas BK, Dogan L, et al. Is there any relationship between adc values of diffusion-weighted imaging and the histopathological prognostic factors of invasive ductal carcinoma? *Br J Radiol* 2018;91:20170705

15. Catalano OA, Horn GL, Signore A, Iannace C, Lepore M, Vangel M, et al. PET/MR in invasive ductal breast cancer: correlation between imaging markers and histological phenotype. *Br J Cancer* 2017;116:893-902

16. Chang H, Wang D, Li Y, Xiang S, Yang YX, Kong P, et al. Evaluation of breast cancer malignancy, prognostic factors and molecular subtypes using a continuous-time random-walk MR diffusion model. *Eur J Radiol* 2023;166:111003

17. Chen Y, Wang J, Zhang X, Yang W, Chen H, Bao B, et al. Correlation between apparent diffusion coefficient and pathological characteristics of patients with invasive breast cancer. *Ann Transl Med* 2021;9:143

18. Chen X, Gao Q, Wu Z, Wang H, Wang J. Correlations between dynamic-enhanced magnetic resonance imaging quantitative parameters and postoperative recurrence or metastasis and clinicopathological features in breast cancer patients-a retrospective cohort study. *Gland Surg* 2022;11:1374-1382

19. Cho GY, Moy L, Kim SG, Baete SH, Moccaldi M, Babb JS, et al. Evaluation of breast cancer using intravoxel incoherent motion (IVIM) histogram analysis: comparison with malignant status, histological subtype, and molecular prognostic factors. *Eur Radiol* 2016;26:2547-2558

20. Choi SY, Chang YW, Park HJ, Kim HJ, Hong SS, Seo DY. Correlation of the apparent diffusion coefficiency values on diffusion-weighted imaging with prognostic factors for breast cancer. *Br J Radiol* 2012;85:e474-e479

21. Choi BB, Kim SH, Kang BJ, Lee JH, Song BJ, Jeong SH, et al. Diffusion-weighted imaging and FDG PET/CT: predicting the prognoses with apparent diffusion coefficient values and maximum standardized uptake values in patients with invasive ductal carcinoma. *World J Surg Oncol* 2012;10:126

22. Kamitani T, Matsuo Y, Yabuuchi H, Fujita N, Nagao M, Jinnouchi M, et al. Correlations between apparent diffusion coefficient values and prognostic factors of breast cancer. *Magn Reson Med Sci* 2013;12:193-199

23. Fan M, He T, Zhang P, Cheng H, Zhang J, Gao X, et al. Diffusion-weighted imaging features of breast tumours and the surrounding stroma reflect intrinsic heterogeneous characteristics of molecular subtypes in breast cancer. *NMR Biomed* 2018;31:e3869

24. Feng W, Gao Y, Lu XR, Xu YS, Guo ZZ, Lei JQ. Correlation between molecular prognostic factors and magnetic resonance imaging intravoxel incoherent motion histogram parameters in breast cancer. *Magn Reson Imaging* 2022;85:262-270

25. Guo Y, Kong QC, Li LQ, Tang WJ, Zhang WL, Ning GY, et al. Whole volume apparent diffusion coefficient (ADC) histogram as a quantitative imaging biomarker to differentiate breast lesions: correlation with the Ki-67 proliferation index. *Biomed Res Int* 2021;2021:4970265

26. Horvat JV, Bernard-Davila B, Helbich TH, Zhang M, Morris EA, Thakur SB, et al. Diffusion-weighted imaging (DWI) with apparent diffusion coefficient (ADC) mapping as a quantitative imaging biomarker for prediction of immunohistochemical receptor status, proliferation rate, and molecular subtypes of breast cancer. *J Magn Reson Imaging* 2019;50:836-846

27. Iima M, Kataoka M, Kanao S, Onishi N, Kawai M, Ohashi A, et al. Intravoxel incoherent motion and quantitative non-Gaussian diffusion MR imaging: evaluation of the diagnostic and prognostic value of several markers of malignant and benign breast lesions. *Radiology* 2018;287:432-441

28. Jeh SK, Kim SH, Kim HS, Kang BJ, Jeong SH, Yim HW, et al. Correlation of the apparent diffusion coefficient value and dynamic magnetic resonance imaging findings with prognostic factors in invasive ductal carcinoma. *J Magn Reson Imaging* 2011;33:102-109

29. Karan B, Pourbagher A, Torun N. Diffusion-weighted imaging and (18)F-fluorodeoxyglucose positron emission tomography/computed tomography in breast cancer: correlation of the apparent diffusion coefficient and maximum standardized uptake values with prognostic factors. *J Magn Reson Imaging* 2016;43:1434-1444

30. Kim SH, Cha ES, Kim HS, Kang BJ, Choi JJ, Jung JH, et al. Diffusion-weighted imaging of breast cancer: correlation of the apparent diffusion coefficient value with prognostic factors. *J Magn Reson Imaging* 2009;30:615-620

31. Kim EJ, Kim SH, Park GE, Kang BJ, Song BJ, Kim YJ, et al. Histogram analysis of apparent diffusion coefficient at 3.0t: correlation with prognostic factors and subtypes of invasive ductal carcinoma. *J Magn Reson Imaging* 2015;42:1666-1678

32. Kim Y, Ko K, Kim D, Min C, Kim SG, Joo J, et al. Intravoxel incoherent motion diffusion-weighted MR imaging of breast cancer: association with histopathological features and subtypes. *Br J Radiol* 2016;89:20160140

33. Kitajima K, Yamano T, Fukushima K, Miyoshi Y, Hirota S, Kawanaka Y, et al. Correlation of the SUVmax of FDG-PET and ADC values of diffusion-weighted MR imaging with pathologic prognostic factors in breast carcinoma. *Eur J Radiol* 2016;85:943-949

34. Kitajima K, Miyoshi Y, Yamano T, Odawara S, Higuchi T, Yamakado K. Prognostic value of FDG-PET and DWI in breast cancer. *Ann Nucl Med* 2018;32:44-53

35. Lee YJ, Kim SH, Kang BJ, Kang YJ, Yoo H, Yoo J, et al. Intravoxel incoherent motion (IVIM)-derived parameters in diffusion-weighted MRI: associations with prognostic factors in invasive ductal carcinoma. *J Magn Reson Imaging* 2017;45:1394-1406

36. Tuan Linh L, Minh Duc N, Minh Duc N, Tra My TT, Viet Bang L, Cong Tien N, et al. Correlations between apparent diffusion coefficient values and histopathologic factors in breast cancer. *Clin Ter* 2021;172:218-224

37. Liu F, Wang M, Li H. Role of perfusion parameters on DCE-MRI and ADC values on DWMRI for invasive ductal carcinoma at 3.0 tesla. *World J Surg Oncol* 2018;16:239

38. Martincich L, Deantoni V, Bertotto I, Redana S, Kubatzki F, Sarotto I, et al. Correlations between diffusion-weighted imaging and breast cancer biomarkers. *Eur Radiol* 2012;22:1519-1528

39. Molinari C, Clauser P, Girometti R, Linda A, Cimino E, Puglisi F, et al. MR mammography using diffusion-weighted imaging in evaluating breast cancer: a correlation with proliferation index. *Radiol Med* 2015;120:911-918

40. Mori N, Ota H, Mugikura S, Takasawa C, Ishida T, Watanabe G, et al. Luminal-type breast cancer: correlation of apparent diffusion coefficients with the Ki-67 labeling index. *Radiology* 2015;274:66-73

41. Nakajo M, Kajiya Y, Kaneko T, Kaneko Y, Takasaki T, Tani A, et al. FDG PET/CT and diffusion-weighted imaging for breast cancer: prognostic value of maximum standardized uptake values and apparent diffusion coefficient values of the primary lesion. *Eur J Nucl Med Mol Imaging* 2010;37:2011-2020

42. Okuma H, Sudah M, Kettunen T, Niukkanen A, Sutela A, Masarwah A, et al. Peritumor to tumor apparent diffusion coefficient ratio is associated with biologically more aggressive breast cancer features and correlates with the prognostication tools. *PLoS One* 2020;15:e0235278

43. Orguc S, Açar ÇR. Correlation of shear-wave elastography and apparent diffusion coefficient values in breast cancer and their relationship with the prognostic factors. *Diagnostics (Basel)* 2022;12:3021

44. Park SH, Choi HY, Hahn SY. Correlations between apparent

diffusion coefficient values of invasive ductal carcinoma and pathologic factors on diffusion-weighted MRI at 3.0 tesla. *J Magn Reson Imaging* 2015;41:175-182

45. Qin Y, Wu F, Hu Q, He L, Huo M, Tang C, et al. Histogram analysis of multi-model high-resolution diffusion-weighted MRI in breast cancer: correlations with molecular prognostic factors and subtypes. *Front Oncol* 2023;13:1139189

46. Qin Y, Tang C, Hu Q, Zhang Y, Yi J, Dai Y, et al. Quantitative assessment of restriction spectrum MR imaging for the diagnosis of breast cancer and association with prognostic factors. *J Magn Reson Imaging* 2023;57:1832-1841

47. Qin Y, Tang C, Hu Q, Yi J, Yin T, Ai T. Assessment of prognostic factors and molecular subtypes of breast cancer with a continuous-time random-walk MR diffusion model: using whole tumor histogram analysis. *J Magn Reson Imaging* 2023;58:93-105

48. Ren C, Zou Y, Zhang X, Li K. Diagnostic value of diffusion-weighted imaging-derived apparent diffusion coefficient and its association with histological prognostic factors in breast cancer. *Oncol Lett* 2019;18:3295-3303

49. Roknsharifi S, Fishman MDC, Agarwal MD, Brook A, Kharbanda V, Dialani V. The role of diffusion weighted imaging as supplement to dynamic contrast enhanced breast MRI: can it help predict malignancy, histologic grade and recurrence? *Acad Radiol* 2019;26:923-929

50. Sharma U, Sah RG, Agarwal K, Parshad R, Seenu V, Mathur SR, et al. Potential of diffusion-weighted imaging in the characterization of malignant, benign, and healthy breast tissues and molecular subtypes of breast cancer. *Front Oncol* 2016;6:126

51. Shen L, Zhou G, Tong T, Tang F, Lin Y, Zhou J, et al. ADC at 3.0 T as a noninvasive biomarker for preoperative prediction of Ki67 expression in invasive ductal carcinoma of breast. *Clin Imaging* 2018;52:16-22

52. Shin HJ, Kim SH, Lee HJ, Gong G, Baek S, Chae EY, et al. Tumor apparent diffusion coefficient as an imaging biomarker to predict tumor aggressiveness in patients with estrogen-receptor-positive breast cancer. *NMR Biomed* 2016;29:1070-1078

53. Suo S, Zhang D, Cheng F, Cao M, Hua J, Lu J, et al. Added value of mean and entropy of apparent diffusion coefficient values for evaluating histologic phenotypes of invasive ductal breast cancer with MR imaging. *Eur Radiol* 2019;29:1425-1434

54. Suo S, Cheng F, Cao M, Kang J, Wang M, Hua J, et al. Multiparametric diffusion-weighted imaging in breast lesions: association with pathologic diagnosis and prognostic factors. *J Magn Reson Imaging* 2017;46:740-750

55. Tang WJ, Jin Z, Zhang YL, Liang YS, Cheng ZX, Chen LX, et al. Whole-lesion histogram analysis of the apparent diffusion coefficient as a quantitative imaging biomarker for assessing the level of tumor-infiltrating lymphocytes: value in molecular subtypes of breast cancer. *Front Oncol* 2021;10:611571

56. Tezcan Ş, Uslu N, Öztürk FU, Akçay EY, Tezcaner T. Diffusion-weighted imaging of breast cancer: correlation of the apparent diffusion coefficient value with pathologic prognostic factors.

Eur J Breast Health 2019;15:262-267

57. Tanişman Ö, Kiziltepe FT, Yildirim Ç, Coşar ZS. Prediction of prognostic factors in breast cancer: a noninvasive method utilizing histogram parameters derived from ADC maps. *Heliyon* 2023;9:e16282

58. Wang Z, Ren GY, Yin Q, Wang Q. Correlation of magnetic resonance imaging quantitative parameters and apparent diffusion coefficient value with pathological breast cancer. *World J Clin Cases* 2022;10:7333-7340

59. Yang Z, Chen X, Zhang T, Cheng F, Liao Y, Chen X, et al. Quantitative multiparametric MRI as an imaging biomarker for the prediction of breast cancer receptor status and molecular subtypes. *Front Oncol* 2021;11:628824

60. Yuan C, Jin F, Guo X, Zhao S, Li W, Guo H. Correlation analysis of breast cancer DWI combined with DCE-MRI imaging features with molecular subtypes and prognostic factors. *J Med Syst* 2019;43:83

61. Zhao M, Fu K, Zhang L, Guo W, Wu Q, Bai X, et al. Intravoxel incoherent motion magnetic resonance imaging for breast cancer: a comparison with benign lesions and evaluation of heterogeneity in different tumor regions with prognostic factors and molecular classification. *Oncol Lett* 2018;16:5100-5112

62. Zhuang Z, Zhang Q, Zhang D, Cheng F, Suo S, Geng X, et al. Utility of apparent diffusion coefficient as an imaging biomarker for assessing the proliferative potential of invasive ductal breast cancer. *Clin Radiol* 2018;73:473-478

63. Meyer HJ, Wienke A, Surov A. Diffusion-weighted imaging of different breast cancer molecular subtypes: a systematic review and meta-analysis. *Breast Care (Basel)* 2022;17:47-54

64. Someya Y, Iima M, Imai H, Yoshizawa A, Kataoka M, Isoda H, et al. Investigation of breast cancer microstructure and microvasculature from time-dependent DWI and CEST in correlation with histological biomarkers. *Sci Rep* 2022;12:6523

65. Partridge SC, Zhang Z, Newitt DC, Gibbs JE, Chenevert TL, Rosen MA, et al. Diffusion-weighted MRI findings predict pathologic response in neoadjuvant treatment of breast cancer: the ACRIN 6698 multicenter trial. *Radiology* 2018;289:618-627

66. Li Z, Li X, Peng C, Dai W, Huang H, Li X, et al. The diagnostic performance of diffusion kurtosis imaging in the characterization of breast tumors: a meta-analysis. *Front Oncol* 2020;10:575272

67. Iima M. Perfusion-driven intravoxel incoherent motion (IVIM) MRI in oncology: applications, challenges, and future trends. *Magn Reson Med Sci* 2021;20:125-138

68. Kim JY, Kim JJ, Hwangbo L, Kang T, Park H. Diffusion-weighted imaging of invasive breast cancer: relationship to distant metastasis-free survival. *Radiology* 2019;291:300-307

69. Honda M, Iima M, Kataoka M, Fukushima Y, Ota R, Ohashi A, et al. Biomarkers predictive of distant disease-free survival derived from diffusion-weighted imaging of breast cancer. *Magn Reson Med Sci* 2023;22:469-476

70. Goto M, Le Bihan D, Yoshida M, Sakai K, Yamada K. Adding a model-free diffusion MRI marker to BI-RADS assessment

improves specificity for diagnosing breast lesions. *Radiology* 2019;292:84-93

71. Goto M, Le Bihan D, Sakai K, Yamada K. The diffusion MRI signature index is highly correlated with immunohistochemical status and molecular subtype of invasive breast carcinoma. *Eur Radiol* 2022;32:4879-4888